

Novel Malachite Green- and Rhodamine B-labeled cationic chain transfer agents for RAFT polymerization

Mariana Beija^{a,b,2}, Carlos A.M. Afonso^{b,*,3}, José Paulo S. Farinha^b, Marie-Thérèse Charreyre^{a,*,1}, José M.G. Martinho^{b,*}

^a Unité Mixte CNRS-bioMérieux, École Normale Supérieure de Lyon, 46 Allée d'Italie, 69364 Lyon, Cedex 07, France

^b Centro de Química-Física Molecular and IN - Institute of Nanoscience and Nanotechnology, Instituto Superior Técnico, Av. Rovisco Pais 1, 1049-001 Lisbon, Portugal

ARTICLE INFO

Article history:

Received 7 July 2011

Received in revised form

23 September 2011

Accepted 20 October 2011

Available online 25 October 2011

Keywords:

RAFT polymerization

Dye-labeled polymers

N,N-dimethylacrylamide

ABSTRACT

Two novel cationic RAFT agents have been synthesized, one labeled with a Malachite Green (MG) dye and another with a Rhodamine B (RhoB) dye. MG-labeled dithiobenzoate (MGEDBA) was prepared in a straightforward manner after synthesis of MG-ethylammonium chloride that reacted with a precursor dithiobenzoate bearing an activated ester function. However, the analogous reaction with RhoB amino derivative led to a mixture of dithiobenzoate and thioamide derivatives. An alternative approach yielded the RhoB-labeled RAFT agent (RhoBEDBA) with complete conversion. The purification of these dye-labeled RAFT agents was very challenging because of their dual nature (aromatic and ionic). Both MGEDBA and RhoBEDBA were efficient RAFT chain transfer agents to control the polymerization of *N,N*-dimethylacrylamide (DMA). The resulting α -end-labeled MG- and RhoB-PDMA samples presented low dispersities ($\mathcal{D} < 1.2$) and both chain-ends were preserved. Finally, we showed that the attachment of RhoB and MG to the PDMA polymer chain-end did not influence the photophysical properties of these dyes. Therefore, these new dye-labeled RAFT agents can be used to prepare various labeled polymers and especially water-soluble ones, to study their conformation and dynamics in solution or at interfaces using fluorescence methods, or as labeled probes for imaging and/or diagnosis purposes.

© 2011 Elsevier Ltd. All rights reserved.

1. Introduction

Dye-labeling of polymers is a useful strategy in macromolecular science, both to study chain dynamics including coil-to-globule transitions [1], intra- and inter-molecular associations [2,3], end-to-end cyclizations [4] or conformations of polymer chains in thin films [5], and for applications such as imaging [6,7], signal amplification for diagnostic tests [8] and light-harvesting or antennae [9]. Knowing the exact location of the dye along the polymer chain is a key point in several of these studies. Therefore, dye-labeling at specific positions such as the polymer chain-end (α or ω) or the junction between blocks

is highly desirable [10], especially for the determination of distances at the macromolecular level using fluorescence techniques such as non-radiative Förster Resonance Energy Transfer (FRET) [11].

Recently, with the advances in controlled radical polymerization (CRP) methods, it has been possible to prepare a large range of polymers with not only controlled molecular weight and architecture but also precise end-group functionality. Among these techniques, the reversible addition-fragmentation chain transfer (RAFT) [12,13] polymerization is one of the most versatile. RAFT polymerization can be described as a conventional free radical polymerization that is conducted in the presence of a suitable chain transfer agent (CTA) from the family of thiocarbonylthio compounds (with the general formula $Z-C(=S)-SR$). It operates on the principle of degenerative chain transfer, in which a rapid equilibrium between propagating and dormant chains is established, leading to the same probability of growth of all chains, hence yielding well-defined polymers. An important feature of polymer chains synthesized by RAFT polymerization is the presence of the R and Z groups from the original CTA at their α - and ω -ends, respectively (with the exception of symmetric trithiocarbonates, in which Z is in the middle of the chain).

A widespread methodology for labeling RAFT polymers takes advantage of the terminal thiocarbonylthio moiety [14], that can be

* Corresponding authors. Tel.: +33 (0) 4 72 72 89 38; fax: +33 (0) 4 72 72 87 87.

E-mail addresses: carlosafonso@ff.ul.pt (C.A.M. Afonso), marie-therese.charreyre@ens-lyon.fr (M.-T. Charreyre), jgmartinho@ist.utl.pt (J.M.G. Martinho).

¹ Present address: Laboratoire Joliot-Curie, USR CNRS3010, ENS de Lyon, 46 Allée d'Italie, 69364 Lyon, Cedex 07, France and Laboratoire Ingénierie des Matériaux Polymères, UMR CNRS5223, INSA-Lyon, 69621 Villeurbanne Cedex, France.

² Present address: Centre for Advanced Macromolecular Design (CAMD), School of Chemical Engineering, UNSW, Sydney, NSW 2052, Australia.

³ Present address: Faculty of Pharmacy, University of Lisbon, Av. Prof. Gama Pinto, 1649-019 Lisbon, Portugal.

converted into a thiol through aminolysis [15,16] or reduction [17,18]. Then, reaction with a dye derivative bearing a complementary function (such as maleimide [15,17] or iodide [18]) is carried out, leading to dye-end-labeled polymers. However, large amounts of dye derivatives have usually to be used, especially for long polymer chains (otherwise low labeling yields are expected), implying large costs.

Another common strategy consists in the use of dye-labeled CTAs (modified either at R or Z). Several kinds of CTAs bearing dyes, such as naphthalene [19,20], acenaphthylene [21], anthracene [9,22–24], phenanthrene [25,26], pyrene [27], diphenylanthracene [28], carbazole [29–31], indole [31], spirooxazine [32], naphthalenesulfonate [33], coumarin [34] or Ru(II) polypyridine [35,36], can be found in the literature as recently reviewed by Beija et al. [10]. In order to limit the possibility of dye loss in the final polymer, the link between the dye and the polymer has to be sufficiently robust. However, many of the above examples correspond to Z-modified CTAs that are very sensitive since the dithioester linkage can be easily degraded by hydrolysis, nucleophilic attack and radical mechanisms. In addition, some of the R-modified CTAs present an ester linkage, fragile in basic aqueous media.

Moreover, in all these examples (with the exception of naphthalenesulfonate), only hydrophobic dyes have been employed (mainly from the family of polycyclic aromatic hydrocarbons). This is a limitation for water-soluble polymers, since it is known that the presence of a dye attached to a polymer chain can induce important changes in polymer chain conformation and properties [37] especially in aqueous solutions. In addition, hydrophobic dyes tend to form dimers, causing significant changes on the photophysical properties of the labeled polymer chains. Although desirable for labeling water-soluble polymers, the synthesis of hydrophilic dye-labeled RAFT agents is indeed very challenging. Usually, water-soluble dyes are ionic aromatic molecules, thus amphiphilic in nature, which renders their purification extremely difficult.

From a photophysical point of view, most of the dyes used for the synthesis of RAFT agents absorb in the UV. Nevertheless, for biomedical applications such as imaging or fluorescence detection, it is desirable to have dyes that absorb in the visible or near-infrared (NIR) wavelength range, where light penetration in tissues is deeper while being less harmful to cells.

Here, we present the synthesis of two novel R-modified CTAs functionalized with the dyes Rhodamine B (RhoB) and Malachite Green (MG) through a robust amide bond, and their application for the synthesis of α -dye-labeled poly(*N,N*-dimethyl acrylamide) (PDMA) polymer chains. Both of these dyes are cationic, thus water-soluble. RhoB absorbs and emits in the red ($\lambda_{em}^{max} = 572$ nm), presenting a high fluorescence quantum yield ($\phi_F = 0.53$) [38]. MG is a non-fluorescent dye under common experimental conditions that shows a high molar absorption coefficient ($\lambda_{abs}^{max} = 616.5$ nm; $\epsilon_{abs}^{max} = 148\,900$) [39]. Besides, rhodamine and MG dyes form an excellent donor/acceptor pair for FRET studies, presenting a high Förster critical radius (around 61 Å) [40]. Another advantage of this pair is that MG is a non-fluorescent probe, avoiding the contamination of rhodamine emission and leading to a dark background, which is an ideal situation for both photophysical studies and imaging purposes. Thus, this pair has been used for the surface characterization of polymer nanoparticles [41,42] and to study DNA hybridization on the surface of thermoresponsive polymer nanoparticles [43–45]. To the best of our knowledge, this is the first time that the synthesis of cationic dye-labeled CTAs suitable for RAFT polymerization, absorbing in the visible region of electromagnetic spectrum and forming a FRET donor/acceptor pair is described. These new dye-labeled RAFT agents open up the possibility to design several polymer architectures and to further investigate by FRET (and other fluorescence techniques) their dynamics in

solution or on surfaces and interfaces. Indeed, we used the RhoB-labeled CTA to synthesize RhoB α -end-labeled thermosensitive block copolymers via the RAFT process. Then, we studied the phase separation in Langmuir–Blodgett films of these copolymers. The changes in the film structure could be very well characterized by laser scanning confocal fluorescence microscopy which had not been possible using atomic force microscopy [46]. In the present paper, we focus on the synthesis of the MG- and RhoB-labeled CTAs, their behavior in RAFT polymerization and the photophysical characteristics of both the dye-labeled CTAs and the resulting α -end-labeled PDMA homopolymers.

2. Experimental section

2.1. Materials

Rhodamine B (95%, Sigma) and 4,4'-bis(dimethylamino)benzophenone (Michler's ketone; 98%, Aldrich) were used as received. Before each use, *n*-butyllithium (*n*-BuLi) was titrated with menthol and 2,2'-dipyridyl in dry THF. *N,N*-dimethylacrylamide (DMA) was obtained from Aldrich (99%) and purified by distillation at 24 °C and 0.4 mbar in the presence of hydroquinone. The initiator 2,2'-azobis(isobutyronitrile) (AIBN) (Fluka, 98%) was purified by recrystallization from ethanol. All other reactants were purchased from Aldrich and used without further purification. Synthesis grade solvents were distilled before use. Tetrahydrofuran (THF), dichloromethane and *N,N*-diisopropylethylamine (DIPEA) were dried by distillation under argon in the presence of CaH₂. Dimethylsulfoxide (DMSO) (Aldrich, anhydrous, 99.9%), *N,N*-dimethylformamide (DMF) (Fluka, 99.9%), chloroform-*d* (CDCl₃; +1% TMS, SDS), acetone-*d*₆ (SDS), methanol-*d*₄ (Aldrich), deuterium oxide (D₂O; Aldrich, 99.9%, 0.75 wt% TSP), DMSO-*d*₆ (Aldrich, 99.96%), lithium bromide (Merck) were used as received. The CTAs succinimidoxycarbonyl ethyldithiobenzoate (SEDB, **1**) [47] and *tert*-butyl dithiobenzoate (*t*BDB) [48] were synthesized according to reported procedures.

Flash column chromatography was performed with silica gel 60 (0.040–0.063 mm) purchased from Merck and MN Alugram® SIL G/UV₂₅₄ plates were used for analytical thin layer chromatography. The plates were visualized at 254 nm or at 430 nm (for rhodamine derivatives). All reactions were carried out under argon or nitrogen atmosphere and glass material was oven dried at 120 °C prior to use.

2.2. Synthesis of dye-labeled CTAs

2.2.1. Malachite Green-labeled CTA

2.2.1.1. Malachite Green-ethylammonium chloride (**2**). *p*-bromophenylethyl-1-amine (100 μ L, 129 mg, 0.65 mmol) was dissolved in dry THF (4 mL) and cooled to –78 °C. A solution of *n*-BuLi (1.3 mmol) was then added dropwise and after ca. 60% of addition, a white precipitate was formed. The reaction mixture was stirred for 2 h. Subsequently, a solution of Michler's ketone (86.6 mg, 0.32 mmol) in dry THF (4 mL) was added dropwise and the reaction mixture was let to react overnight. The reaction was quenched by addition of concentrated HCl aqueous solution. The aqueous layer was washed with hexane (3 \times 20 mL) and the water was further removed by evaporation under vacuum. Precipitation from ethanol in diethyl ether yielded 146 mg of **2** as a highly hygroscopic green solid compound.

(See Supporting Information, Table S1, for assignment)

¹H NMR (300 MHz, methanol-*d*₄): δ (ppm) = 3.00 (t, 2H₆, *J* = 7.1 Hz), 3.14 (t, 2H₇, *J* = 7.4 Hz), 3.28 (s, 12H₁), 6.97–7.82 (m, 4H₂, 4H₃, 2H₄, 2H₅).

¹³C NMR (75 MHz, methanol-*d*₄): δ (ppm) = 33.79 (C₁₁), 34.36 (C₁₂), 41.09 (C₁), 114.86 (C₃), 116.93 (not assigned), 121.67, 128.18,

128.45 (C_q), 129.80, 129.93, 130.30, 130.82, 131.55, 131.87, 132.96, 133.17, 136.32, 137.98 (C_q), 139.92 (C_q) 141.88, 158.48 (C₆).

MS (ESI): m/z (%) = 424.5 (15.7), 372.2 (54.1) [(M-H)⁺], 333.08 (16.7), 295.2 (58.2), 269.2 (100), 253.2 (31.3).

HRMS (ESI): m/z calcd for C₂₅H₃₀N₃: 372.2434, found: 372.2442.

2.2.1.2. Malachite Green ethyl dithiobenzoate amide (MGEDBA, 3). To a stirred solution of SEDB (**1**, 206.9 mg, 0.64 mmol) and DIPEA (230 μ L, 171.2 mg, 1.32 mmol) in anhydrous DMF (30 mL), a solution of MG-ethylammonium chloride (279.7 mg, 0.63 mmol) in DMF was added dropwise at 30 °C. After 2 h 30 min, additional DIPEA (150 μ L, 111.3 mg, 0.86 mmol) was added and the reaction mixture was stirred overnight. After solvent removal, the mixture was chromatographed on a silica gel column (eluent: CH₃CN/H₂O 10:0 to 9:1) to afford 199 mg of **3** as a green product.

¹H NMR (200 MHz, DMSO-*d*₆; see supporting information, Figure S1): δ (ppm) = 1.51 (d, 3H₅, J = 7.1 Hz); 3.11–3.15 (m, 2H₆); 3.29 (s, 12H₁); 3.53–3.63 (m, 2H₇); 4.59 (q, 1H₄, J = 7.0 Hz); 7.03–7.66 (m), 7.87–7.91 (m) (4H₂, 4H₃, 2H₄, 2H₅, 1H₁, 2H₂, 2H₃).

¹³C NMR (50 MHz, CDCl₃; see supporting information, Figure S2): δ (ppm) = 16.76 (C₇); 38.73 (C₁₁); 40.55 (C₁₂); 41.04 (C₁); 111.71, 113.58 (C₃); 126.97, 127.09, 127.24, 128.03, 128.31, 128.39, 128.44, 128.76, 129.43, 130.88, 135.22, 137.38 (C₄, C₅, C₇–C₁₀, C₁–C₃); 144.31 (C₄); 146.17, 149.44 (C₂); 156.81 (C₆); 170.78 (C₁₃); 227.08 (C₁₆). Note: It is probable that C₄ and C₅ present more than one peak.

MS (ESI; see supporting information, Figure S3): m/z (%) = 580.2 (100) [M⁺], 564.2 (17) [(M-S+O)⁺], 476.2 (16).

2.2.2. Rhodamine B-labeled CTA

2.2.2.1. Rhodamine B lactone.

Followed reported procedure [49]. Rhodamine B (1.5 g, 3.1 mmol) was dissolved in 1 mol L⁻¹ aqueous NaOH solution (100 mL) and stirred for 2 h. Thereafter, it was partitioned with ethyl acetate (75 mL). The organic layer was isolated and the aqueous layer was extracted twice with ethyl acetate (EtOAc). Combined organic layers were washed once with 1 mol L⁻¹ NaOH and then brine. The organic solution was dried with Na₂SO₄, filtered, concentrated under reduced pressure and dried to yield 1.3 g of Rhodamine B lactone as a pink product (94%).

Spectral data similar to those reported (¹H NMR, 300 MHz, methanol-*d*₄) [49].

(See Supporting Information, Table S1, for assignment)

¹H NMR (300 MHz, acetone-*d*₆): δ (ppm) = 1.15 (t, 12H₁, J = 7.0 Hz), 3.41 (q, 8H₂, J = 7.0 Hz), 6.43 (dd, 2H₄, J = 2.6, 8.7 Hz), 6.46 (d, 2H₃, J = 2.3 Hz), 6.54 (d, 2H₅, J = 8.7 Hz), 7.23 (br d, 1H₉, J = 7.5 Hz), 7.68 (ddd, 1H₇, J = 1.0, 7.4, 7.4 Hz), 7.76 (ddd, 1H₈, J = 1.2, 7.4, 7.4 Hz), 7.96 (br d, 1H₆, J = 7.4 Hz).

¹³C NMR (75 MHz, acetone-*d*₆): δ (ppm) = 13.78 (C₁), 45.92 (C₂), 86.46 (C₉), 99.15 (C₄), 107.91 (C₆), 109.95 (C₈), 125.91, 126.01, 129.57, 130.56, 131.29, 136.54, 151.27, 154.96, 155.92, 170.66 (C₁₆).

2.2.2.2. Rhodamine B piperazine amide (**4**).

Followed reported procedure [49]. A 2 mol L⁻¹ solution of trimethyl aluminium in hexanes (2 mL, 4.08 mmol) was added dropwise to a solution of piperazine (707.9 mg, 8.2 mmol) in dry dichloromethane (4.5 mL). The reaction mixture was stirred for 1 h until formation of a white precipitate. Then, a solution of Rhodamine B lactone (903.5 mg, 2.04 mmol) was added dropwise to the previous mixture. After reacting under reflux for 24 h, the mixture was quenched by addition of a 0.1 mol L⁻¹ HCl aqueous solution. The heterogeneous solution was filtered and the retained solids were washed with dichloromethane and then with a mixture dichloromethane/methanol (4:1). The combined filtrate was concentrated, resolubilized in dichloromethane, filtered to remove exceeding salt and reconcentrated. The

obtained solid was partitioned between EtOAc and a diluted solution of NaHCO₃. The aqueous layers were combined and washed three times with EtOAc to remove the remaining Rhodamine B lactone, then saturated with NaCl and acidified with 1 mol L⁻¹ HCl. Rhodamine B piperazine amide was extracted several times with a mixture of dichloromethane/*i*-propanol (2:1) until a faint pink color persisted in the aqueous layer. The combined organic layers were dried over Na₂SO₄, filtered and concentrated under reduced pressure. After precipitation in diethyl ether from a methanol solution, 617.5 mg of **4** was recovered by filtration as a dark purple solid (52%).

Spectral data similar to those reported (¹H NMR, 500 MHz, methanol-*d*₄ and ¹³C NMR, 100 MHz, methanol-*d*₄) [49]. (See Supporting Information, Table S1, for assignment.)

¹H NMR (300 MHz, methanol-*d*₄): δ (ppm) = 1.34 (t, 12H₁, J = 7.0 Hz), 3.15 (br s, 4H₁₁), 3.69–3.74 (m, 8H₂ and 4H₁₀), 7.00 (d, 2H₃, J = 1.9 Hz), 7.12 (dd, 2H₄, J = 1.8, 9.5 Hz), 7.29 (d, 2H₅, J = 9.5 Hz), 7.54–7.57 (m, 1H₉), 7.77–7.84 (m, 1H₆, 1H₇, 1H₈).

¹³C NMR (75 MHz, methanol-*d*₄): δ (ppm) = 12.93 (C₁), 44.31, 45.70 (C₁₇, C₁₈), 46.98 (C₂), 97.43 (C₄), 114.85 (C₆), 115.55 (C₈), 128.93, 131.45, 131.65, 131.92, 132.48, 133.06, 135.63, 156.73, 157.26, 159.26, 169.52 (C₁₆).

MS (ESI): m/z (%) = 511.2 (100) [(M-H)⁺].

2.2.2.3. Rhodamine B ethyl dithiobenzoate amide (RhoBEDBA, **5**).

Method 1: A solution of Rhodamine B piperazine amide (91.5 mg, 0.16 mmol) and DIPEA (55 μ L, 0.32 mmol) in dichloromethane was added dropwise to a solution of SEDB (**1**, 51.1 mg, 0.16 mmol) in dichloromethane (20 mL) and the mixture stirred for 18 h at 30 °C. Then, it was washed with acidified water (3 \times 40 mL), dried over Na₂SO₄, filtered and the solvent was evaporated. The obtained solid was redissolved in methanol and precipitated by the addition of diethyl ether. After filtration, 71.8 mg of a dark purple solid were recovered. Characterization techniques showed also the presence of RhoB piperazine thioamide (**6**) with a molar fraction of 50% (yield of **5**: 31%; see spectral data of pure **5** in method 2).

MS (ESI) of the mixture of **5** and **6**: m/z (%) = 719.2 (100) [**5**, M⁺], 703.1 (16) [**6**, (M-S+O)⁺], 631.2 (67) [**6**, M⁺]

Method 2: Rhodamine B piperazine amide (198.5 mg, 0.34 mmol) and DIPEA (150 μ L, 0.86 mmol, 2.5 eq) were dissolved in dry dichloromethane (5 mL). Then, α -bromopropanoyl bromide was added dropwise to previous solution at 0 °C during 10 min. After reacting for 2 h 30 min, the reaction mixture was diluted with dichloromethane (20 mL), washed with saturated Na₂CO₃ solution (3 \times 40 mL, pH ~ 12), then with saturated NH₄Cl solution (40 mL), dried (Na₂SO₄), filtered and concentrated under vacuum to afford 185 mg of Rhodamine B halopropanamide (**7**) as a dark purple solid (mixture 1:1 of bromo- and chloro- derivatives calculated by ¹H NMR; 82% yield).

(See supporting information, Table S1, for assignment).

¹H NMR (200 MHz, acetone-*d*₆): δ (ppm) = 1.26 (t, 12H₁, J = 5.5 Hz), 1.51 (d, 3H₅, X = Cl, J = 6.4 Hz), 1.62 (d, 3H₅, X = Br, J = 6.9 Hz), 3.16 (br s, 4H₁₁), 3.38–3.54 (m, 4H₁₀), 3.73–3.77 (br m, 8H₂), 4.18 (q, 1H₄, X = Br, J = 7.1 Hz), 4.55 (q, 1H₄, X = Cl, J = 6.9 Hz), 6.91 (br, 2H₃), 7.28 (br m, 2H₄ and 2H₅), 7.50 (br m, 1H₉), 7.75 (br m, 1H₆, 1H₇, 1H₈).

¹³C NMR (50 MHz, acetone-*d*₆): δ (ppm) = 13.98 (C₁), 22.26 (C₂₁), 42.92, 43.72 (C₁₇, C₁₈), 45.79 (C₄, X = Br), 47.57 (C₂), 56.16 (C₄, X = Cl), 97.73 (C₄), 115.16, 115.29 (C₆), 116.32 (C₈), 129.53, 130.37, 131.47, 131.59, 132.08, 132.96, 133.78, 157.36, 157.52, 157.71, 168.77 (C₁₆), 169.17 (C₈, X = Cl), 170.84 (C₈, X = Br).

MS (ESI): m/z (%) = 601.3 (100) [M(X = ³⁵Cl)⁺], 603.3 (33) [M(X = ³⁷Cl)⁺], 645.1 (20) [M(X = ⁷⁹Br)⁺], 647.1 (20) [M(X = ⁸¹Br)⁺].

Carbon disulfide (220 μ L, 277 mg, 3.6 mmol) was added dropwise to a solution of phenylmagnesium bromide (3.6 mmol) in dry

THF (5.6 mL) at 0 °C. After stirring for 1 h 30, a 2 mol L⁻¹ HCl aqueous solution (4 mL) was added to the reaction mixture and extracted with diethyl ether (10 mL). Sodium dithiobenzoate was extracted from organic layer with a 1 mol L⁻¹ NaOH aqueous solution. The dithiobenzoate concentration was adjusted to 0.2 mol L⁻¹ and the solution pH was adjusted to 6. To a stirred solution containing Rhodamine B propanoyl piperazine amide (185 mg, 0.28 mmol) and a catalytic amount of NaI (15 mg, 0.1 mmol) in 5 mL of dichloromethane, 5 mL of sodium dithiobenzoate solution was added and the mixture was vigorously stirred overnight. The reaction mixture was washed with a borate buffer solution (pH = 9), then brine. The organic layer was dried over Na₂SO₄, filtered and concentrated under reduced pressure. After purification by dissolution in methanol, followed by precipitation in diethyl ether and silica gel chromatography (CH₂Cl₂/methanol 10:0 to 8:2), **5** was obtained as a purple powder in 58% yield.

¹H NMR (300 MHz, acetone-*d*₆, see supporting information, Figure S4): δ(ppm) = 1.29 (t, 12H₁, J = 7.0 Hz), 1.54 (d, 3H₅, J = 6.4 Hz), 2.99 (br s, 4H₁₁), 3.38–3.57 (m, 4H₁₀), 3.76 (br s, 8H₂), 5.09 (q, 1H₄, J = 6.5 Hz), 6.96 (d, 2H₃, J = 2.2 Hz), 7.24 (dd, 2H₄, J = 2.3, 9.5 Hz), 7.34 (d, 2H₅, J = 9.1 Hz), 7.47 (dd, 2H₂, J = 7.6, 7.8 Hz), 7.54–7.58 (m, 1H₉), 7.75–7.80 (m, H₁₂, H₁₃, H₁₄), 7.96 (d, 2H₂₄, J = 7.1 Hz).

¹³C NMR (75 MHz, acetone-*d*₆, see supporting information, Figure S5): δ(ppm) = 13.92 (C₁); 18.26 (C₇); 43.26 (C₁₈); 47.62 (C₂); 48.86, 49.22 (C₁₇, C₆); 97.89 (C₄); 115.45, 115.50 (C₆); 116.33 (C₈); 128.52, 129.65, 131.58, 131.74, 132.23, 133.07, 134.06, 134.77, 137.63, 157.59, 158.15, 159.55 (C₃, C₅, C₇, C₉–C₁₅, C₂₃–C₂₆); 168.83 (C₁₆); 170.19 (C₈); 228.69 (C₅).

MS (ESI): *m/z* (%) = 719.2 (100) [M⁺]

HRMS (FAB, see supporting information, Figure S6): *m/z* calcd for C₄₂H₄₇N₄O₃S₂⁺: 719.308960; found: 719.311351.

2.3. Polymerization procedures

Typically, monomer(s), initiator, solvent, CTA and trioxane (used as internal reference for monomer conversion) were introduced either in an NMR tube fitted with a Young's valve or a Schlenk tube equipped with a magnetic stirrer. The polymerization mixture was then degassed by five freeze-pump-thaw cycles and set under nitrogen atmosphere.

For experiments carried out in an NMR tube, a ¹H NMR spectrum of the mixture was performed at 27 °C prior to polymerization initiation. After removing the NMR tube, the cavity of the magnet was heated at the required temperature and allowed to stabilize for 30 min. The actual temperature was checked by the chemical shift difference of protons of a (80:20) ethyleneglycol:DMSO mixture [50,51]. Afterwards, the NMR tube containing the polymerization mixture was reintroduced and let to equilibrate for 2 min, before the magnet was shimmed. Monomer conversions were periodically (3–15 min) monitored by on-line ¹H NMR spectroscopy.

Alternatively, for experiments carried out in a Schlenk tube, a first sample was withdrawn from the polymerization medium at room temperature and then, polymerization was thermally initiated by introducing the Schlenk tube in a thermostated oil bath at the required temperature. Samples were periodically withdrawn from the polymerization medium and quenched in liquid nitrogen for determination of monomer conversion by ¹H NMR. Usually, 400 μL of chloroform-*d* or acetone-*d*₆ were added to 200 μL of each sample.

Determination of monomer conversion was achieved by comparison between the integral values of the monomer(s) vinyl protons and the trioxane protons (singlet peak, used as internal

reference) at initial polymerization time (*t* = 0) and at polymerization time, *t*.

2.4. Purification of polymer samples

PDMA polymer chains were purified by dialysis using Slide-A-Lyzer® dialysis cassettes from Pierce with a molecular weight cut-off (MWCO) of 3500 Da or 2000 Da (polymers with *M_n* < 10 000 g mol⁻¹). Before dialysis, samples were diluted 10 times with milliQ water in order to have a maximum of 10% v/v DMSO content. Typically, after introduction of the sample, the cassette was left to float in a water bath (500 times the volume of the sample). After 2 h dialysis, water was changed and dialysis proceeded for another 2 h. Afterwards, water was changed again, at least once a day, until all low molecular weight molecules have been removed (confirmation by ¹H NMR and/or SEC analyses). The sample was recovered and freeze-dried in a Lyoalfa 6-80 Telstar (Varian DS 202) equipment.

2.5. Characterization

2.5.1. Nuclear magnetic resonance

¹H and ¹³C NMR spectra were recorded on a Bruker AC 200 spectrometer (200 MHz and 50 MHz, respectively), on a Bruker Avance II (300 MHz and 75 MHz, respectively) and, for polymer characterization, on a Bruker Avance II (400 MHz, 40 °C). Chemical shifts are reported as δ values relative to tetramethylsilane (δ_H = 0 ppm). Signal multiplicities are designed as follows: s – singlet, d – doublet, t – triplet, q – quadruplet, m – multiplet, br – broad.

2.5.2. Mass spectrometry

Low resolution mass spectra were carried out at the Institut de Biologie et Chimie de Protéines (IBCP, Lyon, France) using either electrospray ionization (ESI) or matrix-assisted laser desorption/ionization time-of-flight (MALDI-ToF) mass spectrometry techniques with positive ions detection. ESI mass spectra were recorded on an API 165 (Applied Biosystems) spectrometer (ion spray voltage: 5 kV), using a quadrupole scan speed of 100 Da/s and a flow rate of 5 μL/min; samples were dissolved in methanol/water/formic acid (50/50/0.1). Otherwise, MALDI-ToF mass spectra were recorded on a Voyager DE-PRO (Applied Biosystems) spectrometer with an acceleration voltage of 20 kV and with an extraction delay of 140 ns; α-cyano-4-hydroxycinnamic acid (0.5 mg) dissolved in 100 μL of acetonitrile/water/TFA (50/50/0.1) mixture was used as matrix.

Alternatively, high- and low-resolution mass spectra (Electronic Impact - EI, ESI or Fast Atom Bombardment - FAB) were carried out by the mass spectrometry service of the University of Santiago de Compostela (Spain).

2.5.3. Organic size exclusion chromatography

Polymer samples were characterized by SEC-MALS using a Waters 510 pump fitted with three Phenogel columns (10⁴, 10³ and 10² Å; 5 μm; 7.8 × 300 mm; columns temperature: 35 °C) connected in series and a miniDAWN-treos multi-angle laser light scattering detector (three angles: 45.8°, 90° and 134.2°; laser wavelength: 658 nm) from Wyatt Technologies and a Waters 2410 refractive index detector at 30 °C. Simultaneously, detection of either fluorescence (Waters 478 detector) or absorption (Waters 486 detector) of polymer samples was performed to confirm the existence of the chromophore/fluorophore at the α-chain-end. MG-PDMA samples were observed at an absorption wavelength of 600 nm and RhoB-PDMA samples were detected by fluorescence (λ_{exc} = 560 nm; λ_{em} = 575 nm). A solution of 0.05 M LiBr in DMF

was used as eluent at a flow rate of 0.3 mL min⁻¹. Typically, 50 µL of a sample solution (10 g L⁻¹) was injected in the system. Prior to injection, these solutions were centrifuged at 15 000 rpm for 15 min. Relative molecular weights were obtained using a calibration curve with *N*-succinimidyl propionate-PDMA and *t*-butyl-PDMA samples as PDMA standards.

2.5.4. Determination of specific refractive index increments

The specific refractive index increment (dn/dc) for PDMA was determined in 0.05 M LiBr DMF solution using a WYATT Optilab rEX detector operating at 658 nm and 30 °C (0.0813 ± 0.0005 mL g⁻¹).

2.5.5. Absorption and fluorescence

UV–Visible absorption measurements were performed in a Shimadzu Model 3101 spectrometer and fluorescence spectra were recorded on a SPEX Fluorolog F112A fluorometer (bandwidth of 0.9 nm (excitation) and 0.45 nm (emission)). Emission spectra of RhoB derivatives were obtained between 535 nm and 750 nm, using 530 nm as excitation wavelength. All spectra were obtained with right angle geometry, at room temperature and using quartz cells of 0.5 cm × 0.5 cm.

Fluorescence intensity decay curves, with picosecond resolution, were obtained by the single-photon timing technique using laser excitation of 570 nm. The system consists of a mode-locked Coherent Inova 440-10 argon ion laser synchronously pumping a cavity dumped Coherent 701-2 dye laser using Rhodamine 6G, which delivers 3–4 ps pulses at a repetition rate of 4 MHz. The fluorescence was observed at 585 nm using a polarizer set at the magic angle and a cut-off filter to effectively eliminate the scattered light. The fluorescence was selected by a Jobin-Yvon HR320 monochromator with a grating of 100 lines/mm and detected by a Hamamatsu 2809U-01 microchannel plate photomultiplier. Time-scales of 7–12 ps/channel were used. The decay curves were analyzed using home-made non-linear least-square deconvolution software based on the Marquard algorithm [52]. All measurements were performed at room temperature.

3. Results and discussion

3.1. Synthesis and characterization of dye-labeled CTAs

In order to synthesize the new dye-labeled CTAs, a convergent strategy was chosen involving a coupling reaction between an amino derivative of the dye and a precursor dithioester **1**, according to Scheme 1. This strategy was first developed for the synthesis of bio-related dithiobenzoates carrying a sugar [47], a biotin [47] or a phospholipid [53] and has already been used to get a fluorescent phenanthrene-labeled CTA [26]. However, this is the first time that it is applied to synthesize cationic dye-labeled CTAs, which represents a major challenge. Indeed, very few CTAs of this kind are described in the literature. Prior to the coupling reaction, both MG and RhoB amino derivatives were synthesized since they were not commercially available or analogous were too expensive. Several aspects had to be taken into consideration for the choice of an appropriate synthetic pathway for these dye derivatives: 1) the dye should present a free amino group for further reaction with the precursor dithiobenzoate **1**; 2) a linker should be present between

the amino group and the dye moiety (at least a C₂ group) in order to decrease steric hindrance that could influence the control of the polymerization: indeed, during the pre-equilibrium, while steric hindrance on the R group favors the fragmentation step, it disfavors the addition step (limited access to the thiocarbonylthio group) and the re-initiation step; and 3) the bond between the linker and the dye should be strong, such as a C–C or an amide bond, in order to resist to hydrolysis.

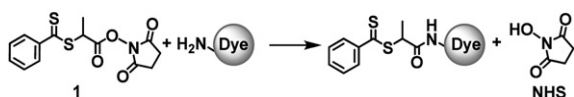
3.1.1. Synthesis of MG-labeled CTA

In the literature, MG derivatives have mainly been synthesized using three methods: Baeyer condensation [54–57], addition of organolithium compounds [55,58–62] or addition of Grignard reagents [55,63]. Often, the second method has been chosen since softer experimental conditions can be employed compared to the first method and higher yields are obtained compared to the latter. Moreover, for our purpose, the introduction of a linker should impart the lowest modifications to the MG spectral properties, which can be achieved with a C–C bond [55]. Then, we decided to synthesize the MG amino derivative by the reaction of Michler's ketone (a commercial compound) and a *p*-functionalized aryllithium compound obtained from a halogen-lithium exchange reaction on a commercial *p*-bromophenylethyl-1-amine (Scheme 2).

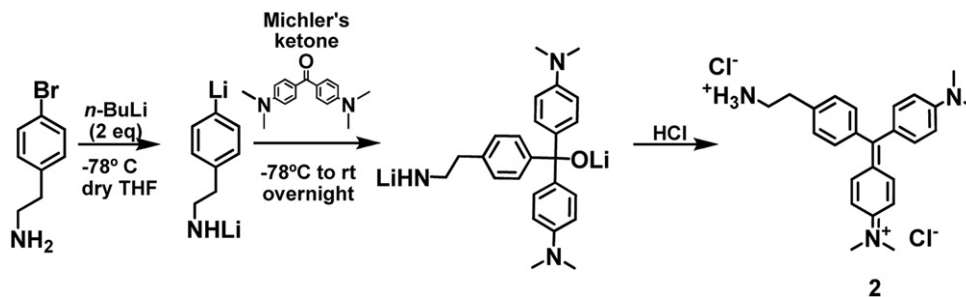
The main advantage of using *p*-bromophenylethyl-1-amine as a reactant was the possibility of preparing directly an amino derivative of MG. Conversely, the presence of a free amino group could favor some side reactions such as the nucleophilic attack of the amine to Michler's ketone. A prior protection of the amino group with a silicon-based protecting group developed by Djuric et al. [64] or with a trityl group was attempted but the MG amino derivative could not be obtained in significant yield. Nonetheless, the MG-ethylammonium chloride **2** was successfully synthesized in a one-pot procedure, without the need to protect the amino group when 2 eq. of *n*-BuLi was added during the halogen-metal exchange step. Indeed, despite the risk of competitive reaction of the amine group with Michler's ketone, the carbanion is much more reactive and the formation of the desired compound is preferred.

The purification of compound **2** was very challenging either when it was isolated as a carbinol (by a neutral work-up) or in chromatic form (by an acid work-up). In the first case, we tried to purify the carbinol using silica gel or reverse-phase chromatography, but it led to degradation of the product. Instead, when the product was precipitated and filtered, we were able to eliminate the residual Michler's ketone, but there were still unidentified impurities in the final product. In the second case, Michler's ketone could be removed by extraction with hexane or diethyl ether from an aqueous solution of **2**. However, it was not possible to find a sufficiently polar eluent to perform a chromatographic purification and recrystallization was unable to eliminate all impurities. It is noteworthy that non-functionalized MG is sold with only 85% purity. Hence, although compound **2** was not completely pure, we decided to perform the reaction with **1** and to purify the resulting MG-labeled CTA.

The coupling between precursor dithioester **1** and MG-ethylammonium chloride **2** was carried out using similar experimental conditions as previously reported (Scheme 3) [53]. Since the MG amino derivative (**2**) was isolated as an ammonium salt, a tertiary amine (*N,N*-diisopropyl ethylamine, DIPEA) was added for deprotonation. Contrary to the previous cases, the reaction was performed in DMF since MG-ethylammonium chloride was only soluble in highly polar solvents (**1** was also very soluble in DMF). Within the first hours of reaction, the formation of a new product could be detected by TLC (new green spot at *R*_f = 0.32, eluent: CH₃CN/H₂O 95:5) and by ¹H NMR [two new peaks could be



Scheme 1. Synthesis of dye-labeled CTAs from a precursor dithioester **1**. NHS: *N*-hydroxysuccinimide.



Scheme 2. Synthesis of MG-ethylammonium chloride (2).

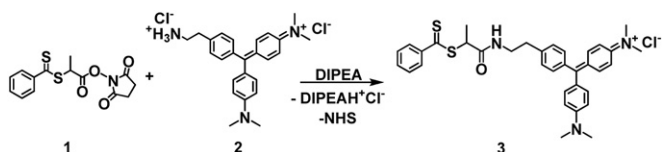
observed: at 1.51 ppm (d) and at 4.59 ppm (q), respectively corresponding to CH_3 and CH of compound **3**].

During purification of MGEDBA (**3**), several difficulties have been encountered due to the strong polarity of this molecule and to the presence of residual impurities from the amino-functionalized dye. Since **3** was soluble in water, elimination of *N*-hydroxysuccinimide (NHS) with water washings was not possible. Therefore, a very polar mixture of solvents (acetonitrile/water) had to be used as eluent for purification by silica gel chromatography to promote migration of MGEDBA (**3**). However, due to the strong polarity of the eluent, some impurities remained in the final product (1H and ^{13}C NMR spectra showed some peaks at high fields). The structure of **3** was confirmed by NMR and ESI-MS analyses (cf. Supporting Information, Figures S1 to S3).

3.1.2. Synthesis of RhoB-labeled CTA

As recently reviewed [65], rhodamine derivatives can be obtained by modification of the amino groups of the xanthenic moiety (position 3 and 6) as well as modification of the carboxyphenyl ring at positions 4' and/or 5' or modification of the carboxylic acid group (position 2'). The first strategy usually leads to loss of fluorescence of the modified dye. With the second strategy, a mixture of products (whose separation is very difficult and time-consuming) is generally obtained. Therefore, we decided to use the third strategy for the synthesis of a rhodamine B (RhoB) amino derivative. As in the case of MG, the RhoB derivative should also have a strong bond (such as a C–C or an amide bond) between the RhoB moiety and the amino group. In addition, the modification should impart no or very little changes on the photophysical properties of the dye. So, we decided to prepare a RhoB piperazine amide derivative using the reaction conditions proposed by Nguyen and Francis [49]. Since this molecule is a tertiary amide, the cyclization to spirolactam [66] (common for secondary amides of rhodamines) is avoided and the fluorescence properties of RhoB are maintained even at basic conditions. The compound **4** (Scheme 4) was successfully obtained with a yield of 52%. After this purification step, the structure of **4** was confirmed by 1H and ^{13}C NMR as well as ESI mass spectrometry (see experimental part) and these analyses indicated a high purity of the product.

Then, the synthesis of RhoB-labeled CTA was first investigated using the same strategy (convergent approach) as for MGEDBA (in dichloromethane with DIPEA as a base for deprotonation). The



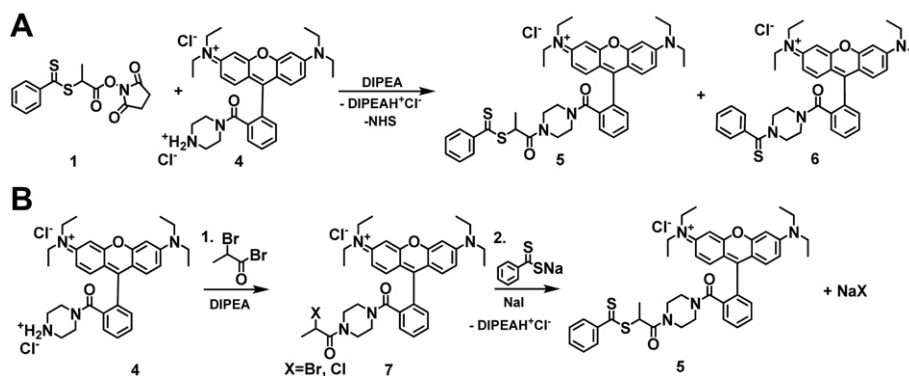
Scheme 3. Synthesis of Malachite Green ethyl dithiobenzoate amide (MGEDBA, **3**). DIPEA: *N,N*-diisopropyl ethylamine; NHS: *N*-hydroxysuccinimide.

reaction was fast, with formation of products within the first minutes as observed on TLC plate (two new spots at $R_f = 0.27$ and 0.33 ; **4** does not migrate and R_f (**1**) = 0.95; eluent: CH_2Cl_2 /Acetone 8:2). DIPEA ammonium salt and NHS as well as remaining **4** (more soluble in water than RhoBEDBA **5** due to the double cationic charge) could be eliminated by washings with acidified water. The final product was then purified by precipitation in diethyl ether from a methanol solution in order to remove the remaining precursor dithioester **1**. However, the purified product contained two rhodamine derivatives: RhoBEDBA (**5**) and a by-product identified as a RhoB piperazine thioamide (**6**) (Scheme 4A) as proved by several evidences: a) 1H NMR spectrum showed a peak at 5.09 ppm (q; by coincidence, at the same chemical shift than the corresponding CH of **1**) and a peak at 1.54 ppm (d; corresponding to protons CH_3 of RhoBEDBA), but the integrals corresponding to aromatic protons and to protons of *N,N*-diethylamino and piperazine groups were two-fold higher than expected; b) ^{13}C NMR spectrum showed, in addition to the peak at 228.7 ppm (characteristic of thiocarbonyl carbon of RhoBEDBA), another peak at 202.6 ppm, which might correspond to a carbon of a C=S bond; c) on the ESI-MS spectrum, two peaks were present, one at $m/z = 719.2$ corresponding to the desired product and another at $m/z = 631.2$ corresponding to the RhoB piperazine thioamide by-product (**6**). **6** was formed upon nucleophilic attack to the dithioester moiety by the amino group of the dye derivative. It was previously demonstrated that this side-reaction did not occur with primary amines if optimal reaction conditions were employed (slow addition of a maximum of one equivalent of amine) [47]. In our case, the dye derivative is a secondary amine and it was estimated by the above three techniques that the final product contained 44–50% of thioamide [67].

The specificity of the nucleophilic attack depends on the relative electrophilicities of each reactive center and the steric hindrance of reactants. The activated ester moiety is more electrophilic than the dithioester moiety. However, secondary amines are more sterically hindered than primary amines and the presence of the methyl group at the β -position relatively to carbonyl may encumber the approach between the secondary amine and the activated ester moiety, decreasing the reactivity of the amine towards this activated ester center.

So, in order to get a pure product, it would be necessary to separate **5** and **6**. However, due to the great similarity between these two structures, it was not possible to find an appropriate eluent for chromatography. Likewise, neither extractions nor recrystallization would be efficient since their solubilities are identical. Hence, a different synthetic strategy was envisioned to obtain a pure RhoBEDBA.

We decided to employ a linear approach (Scheme 4B) similar to the one described by Mertoglu et al. for the synthesis of a naphthalenesulfonate-labeled CTA [33]. In a first step, RhoB bromopropionylpiperazine amide (**7**; X = Br) was prepared by the reaction of



Scheme 4. Synthesis of Rhodamine B ethyl dithiobenzoate amide (RhoBEDBA, 5) by convergent (A) or linear (B) approaches. DIPEA: *N,N*-diisopropyl ethylamine; NHS: *N*-hydroxysuccinimide.

2-bromopropanoyl bromide and **4**, using DIPEA as a base (Scheme B-1). The initial RhoB amino derivative was fully converted within only 1 h 30 min. ¹H NMR analysis showed two quadruplet peaks at 4.18 and 4.55 ppm and two doublet peaks at 1.51 and 1.52 ppm, indicating that two products were formed. ESI-MS analysis confirmed the presence of the desired product (peaks of equal intensities at $m/z = 645.1$ and 647.1 expected for this molecule containing a Br atom). However, a very intense peak at $m/z = 601.3$ and a peak at $m/z = 603.3$ (1/3 of the intensity of the former peak) were also present, corresponding to the same molecule with a chlorine atom (*i.e.* **7** with X = Cl) instead of a bromine one. We suppose that the formation of this product occurred by the concomitant attack of the counter-ion of **4** (Cl⁻) to the carbon at α -position relative to the carbonyl through a S_N2 mechanism. Since Br⁻ is a better leaving group than Cl⁻, the so-formed product would not further react with Br⁻, leading to formation of a RhoB chloropropanoylpiperazine amide (**7**; X = Cl) as the main product. Since both molecules are reactive, such mixture of products was used in the second step of RhoBEDBA synthesis. Moreover, since all reactants and other by-products could be eliminated during washings, no chromatographic purification was carried out at this step. Yields between 80 and 87% were reached.

In the second step, the reaction between **7** and the dithiobenzoate anion is carried out in order to form RhoBEDBA. A biphasic system was used, with solubilization of **7** in dichloromethane (a very good solvent for rhodamine derivatives) and later addition of an aqueous solution (pH = 6) of PhCS₂Na salt (3.5 eq), in the presence of a catalytic amount of NaI to increase the reactivity of the rhodamine halopropanamide derivatives. Using these experimental conditions, it was possible to quantitatively obtain the desired product. RhoBEDBA was first purified by precipitation in diethyl ether from a methanol solution (99% yield). RhoBEDBA was further purified by silica gel chromatography to obtain a highly pure product. However, the yield decreased to 58% since much of the product was lost by adsorption onto the silica (the stationary phase was pinkish at the end of purification). This yield is very close to that obtained by Mertoglu et al. for the synthesis of the naphthalenesulfonate-labeled dithiobenzoate using a linear approach (55%) [33]. The RhoB-labeled CTA was then fully characterized by ¹H NMR, ¹³C NMR and high resolution fast atom bombardment (FAB) mass spectrometry (*cf.* Experimental Section). Those analyses confirmed that a very pure rhodamine-labeled CTA was obtained.

3.2. Homopolymerization of DMA mediated by dye-labeled CTAs

The efficiency of the novel dye-labeled CTAs, MGEDBA (**3**) and RhoBEDBA (**5**), was investigated in the case of the RAFT

homopolymerization of DMA, a bisubstituted acrylamide derivative leading to water-soluble and biocompatible polymers [68,69]. The RAFT polymerization of DMA had been previously studied in our group using *tert*-butyl dithiobenzoate (*t*BDB) as CTA [70,71]. This CTA was very efficient to control the polymerization, giving rise to PDMA chains with experimental number average molecular weights (M_n) close to theoretical values and narrow molecular weight distributions. Moreover, it was previously observed with another acrylamide (*N*-acryloylmorpholine), that no significant differences in kinetics existed when *t*BDB or dithiobenzoates bearing a propanamide derivative as R group were employed [72].

Here, the polymerizations were performed in dimethylsulfoxide (DMSO) since it is a good solvent of DMA, PDMA and both MGEDBA and RhoBEDBA. The dye-labeled CTAs were not soluble enough in water to perform the polymerization in aqueous solution. As mentioned in the introduction, since these dyes are simultaneously aromatic and ionic, they have an amphiphilic nature. So, while they are completely soluble in water at the usual concentrations for fluorescence studies (10^{-7} to 10^{-4} mol L⁻¹), it is not possible to get aqueous solutions at the required concentrations for RAFT polymerization (10^{-3} to 10^{-1} mol L⁻¹). The polymerizations were carried out at 75 °C using AIBN as initiator, with [DMA]₀ = 1.6 mol L⁻¹ and [DMA]₀: [CTA]₀: [AIBN]₀ = 350:1:0.2 (Table 1). Several runs were performed in NMR tubes equipped with a Young's valve in order to monitor the polymerization kinetics by on-line ¹H NMR (in DMSO-*d*₆). Other runs were performed in Schlenk tubes to obtain greater amounts of polymer samples.

First, a reference experiment (run 1) was carried out using *t*BDB in DMSO (previous polymerizations of DMA mediated by *t*BDB had been conducted in 1,4-dioxane [70,71]). Then, under similar experimental conditions, DMA polymerization was undertaken in the presence of MGEDBA (runs 2, 3 and 4) and three different samples of RhoBEDBA (runs 5–9): sample RhoBEDBA-1 synthesized by method A (Scheme 4) with a purity of 53% due to the presence of a thioamide by-product; sample RhoBEDBA-2 synthesized by method B (Scheme 4) and purified by precipitation from methanol in diethyl ether (no impurities were detected in this sample by standard characterization techniques such as ¹H and ¹³C NMR, ESI-MS); and sample RhoBEDBA-3, obtained by further purification by silica gel chromatography of sample RhoBEDBA-2. Although sample RhoBEDBA-1 presented a thioamide by-product, we expected that it should not interfere with the RAFT mechanism since it was previously observed that the polymerization of *n*-butyl acrylate in the presence of an oligopeptide-modified dithiobenzoate containing 24% of a thioamide by-product did not cause any inhibition nor additional retardation [73]. Two runs were carried out with a smaller [DMA]₀: [CTA]₀ ratio (runs 4 and 9, with

Table 1
Experimental conditions of RAFT polymerization of DMA. $T = 75\text{ }^{\circ}\text{C}$; $[\text{CTA}]_0/[\text{AIBN}]_0 = 5$.

Run	CTA Name	Structure	$[\text{DMA}]_0/[\text{CTA}]_0$	$[\text{DMA}]_0$ (mol L ⁻¹)	Solvent
1	tBDB		356	1.6	DMSO- <i>d</i> ₆
2	MGEDBA		351	1.6	DMSO- <i>d</i> ₆
3 ^a	MGEDBA		343	1.6	DMSO
4 ^a	MGEDBA		51	1.0	DMSO
5	RhoBEDBA-1 ^b		354	1.6	DMSO- <i>d</i> ₆
6	RhoBEDBA-2		357	1.4	DMSO- <i>d</i> ₆
7	RhoBEDBA-3		351	1.6	DMSO- <i>d</i> ₆
8 ^a	RhoBEDBA-3		302	1.6	DMSO
9 ^a	RhoBEDBA-3		126	1.6	DMSO

^a Carried out in a Schlenk tube.

^b $[\text{RhoBEDBA-1}]_0$ was corrected taking into account its purity (53%).

MGEDBA and RhoBEDBA-3, respectively) in order to get polymer chains with a lower M_n to facilitate characterization of the α -end group.

The runs that were carried out using RhoBEDBA samples that were not further purified by silica gel chromatography (RhoBEDBA-1 and RhoBEDBA-2) showed an apparent inhibition during the full polymerization time (90 min; Fig. 1; run 5: open circles and run 6: grey circles, respectively). MALDI-ToF MS analyses of the polymerization media demonstrated that this inhibition period was indeed a very long induction period since dormant oligomers bearing the RhoB moiety at the α -chain-end were detected (see supporting information; Figure S7). This long induction period might be caused by the presence of some impurities in the RhoBEDBA-1 and RhoBEDBA-2 samples acting as radical traps. The exact structure of these impurities remains unknown since they were present in very small amounts (not detectable by NMR or MS) but they probably have an ionic aromatic structure close to that of Rhodamine B derivatives which would explain that they were extremely difficult to eliminate. Since this long induction period was also observed in run 6, the thioamide side-product (only present in run 5) was probably not responsible for this effect.

A huge difference was observed when using the RhoBEDBA-3 sample (further purified by silica gel chromatography) in run 7 (Fig. 1; black circles). These results demonstrate that very low amounts of impurities in the CTA sample (run 6, below the detection limit of the characterization techniques) may strongly influence the polymerization kinetics (run 6, 90 min induction period in comparison with run 7, 20 min induction period). Then, when evaluating a new RAFT agent, the occurrence of a long induction period should not only be related to the CTA structure but also to possible traces of impurities in the CTA sample (unless it has been checked carefully). Plummer and co-workers [74] have studied the effect of the presence of impurities in cumyl dithiobenzoate on the polymerization kinetics of 2-hydroxyethyl methacrylate, styrene, and methyl acrylate. They have shown that even the presence of a very low amount of impurity ($\sim 3\%$) may induce partial inhibition or retardation of the polymerization. Moreover, in our group, the

polymerization of NAM in the presence of non purified CTAs ($\sim 25\text{--}39\%$ of impurities) showed additional retardation, which was partially suppressed after meticulous purification of these CTAs (98% purity), with the conversion plateau increasing from 55% to

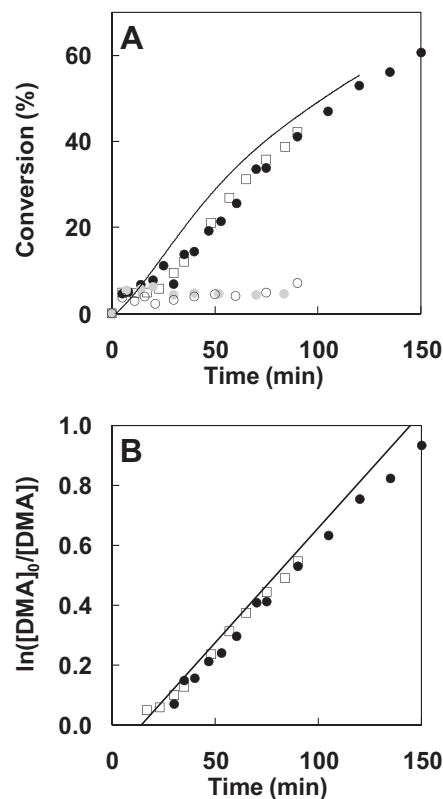


Fig. 1. Time evolution of monomer conversion (A) and pseudo-first order kinetic plots (B) for RAFT polymerization of DMA in DMSO-*d*₆ at 75 °C using tBDB (run 1; solid line), MGEDBA (run 2; □), RhoBEDBA-1 (run 5; ○), RhoBEDBA-2 (run 6; ●) and RhoBEDBA-3 (run 7; ●) as CTA. $[\text{CTA}]_0/[\text{AIBN}]_0 = 5$; $[\text{DMA}]_0/[\text{CTA}]_0 \approx 350$; $[\text{DMA}]_0 = 1.6\text{ mol L}^{-1}$ (except for run 6: $[\text{DMA}]_0 = 1.4\text{ mol L}^{-1}$).

80%. However, besides the presence of these impurities, the molecular weights were generally not affected (dispersities below 1.2, experimental molecular weights very close to the calculated ones taking into account the amount of impurities) [72].

In comparison with the reference experiment with *t*BDB (Fig. 1; run 1: solid line), the rate of polymerization of DMA mediated by RhoBEDBA-3 (Fig. 1; run 7: black circles) was very similar, with ca. 60% DMA conversion reached within 2 h, suggesting that this dithiobenzoate caused a comparable retardation of DMA polymerization, even if a slightly longer induction period was observed (20 min vs. 10–15 min in the case of *t*BDB). This behavior is in agreement with that previously observed with *N*-acryloyl morpholine in the presence of *t*BDB or dithiobenzoates bearing a propanamide derivative as R group [72].

As explained in the previous part, MGEDBA sample contains an important amount of impurities (very difficult to eliminate). Then, the real $[CTA]_0$ was lower than calculated. If we assume that MGEDBA has a similar influence as RhoBEDBA on the RAFT polymerization kinetics (which is a reasonable hypothesis considering that they have the same Z group and a leaving R group of the same nature), and that these impurities are perfectly inert, faster polymerization kinetics (and shorter induction periods) should be observed (Fig. 1, run 2: open squares compared to run 7: black circles). However, since the polymerization rate was almost the same, it is likely that the impurities were not inert. Then, the increase in polymerization rate due to a lower real $[MGEDBA]_0$ might have been balanced by the decrease in polymerization rate caused by the presence of impurities, leading to an apparently similar polymerization rate.

3.3. Characterization of dye-labeled polymer chains and end-group analysis

The α -dye-labeled PDMA chains were characterized by size exclusion chromatography (SEC) in DMF, since this eluent is appropriate for characterization of PDMA samples [75–81] while being a good solvent for both MG and RhoB dyes. Although our apparatus was equipped with a multi-angle light scattering (MALS) detector, it was not possible to obtain the absolute molecular weights of the polymer samples due to optical interference with MG (that absorbs at the laser wavelength with a very high molar absorption coefficient) and RhoB. Although this later should not absorb light at the laser wavelength, a significant response of the MALS detector was observed when RhoBEDBA was analyzed alone. The real reasons for this phenomenon remain unclear but might be related to fluorescence of the RhoB (eventually due to excitation by daylight), which would perturb the light scattering analysis. Therefore, it was necessary to use a calibration curve, obtained with narrow molecular weight distribution PDMA samples synthesized in our laboratory by RAFT polymerization mediated by *tert*-butyl or *N*-succinimidyl dithiobenzoates as CTAs. However, although these PDMA standards have a backbone of the same nature as the MG- and RhoB-labeled PDMA samples, their α -chain-ends are very different. Hence, the α -MG- and α -RhoB-labeled PDMA samples and the PDMA standards may have slightly different conformation in the eluent, thus different hydrodynamic volumes and, accordingly, different retention volumes for polymer chains of the same molecular weight. In addition, α -chain-ends may interact with the stationary phase as previously observed when analyzing α -lipid-functionalized PNAM samples by SEC [53]. Therefore, the experimental M_n values of the α -dye-labeled PDMA samples have to be interpreted with caution.

Size exclusion chromatograms of MG-PDMA and RhoB-PDMA samples (runs 4 and 9, Fig. 2A and B, respectively) are symmetric with the exception of a small shoulder at low retention volumes,

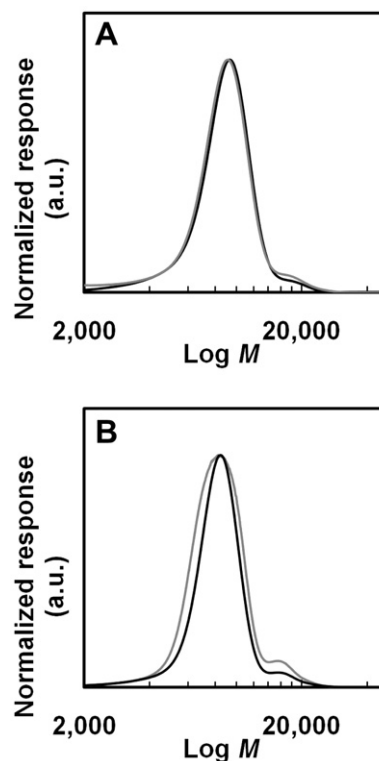


Fig. 2. (A) RI (black line) and UV-Visible (grey line; $\lambda_{\text{abs}} = 600$ nm) traces of MG-PDMA sample obtained in run 4 and (B) RI (black line) and fluorescence (grey line; $\lambda_{\text{exc}} = 560$ nm; $\lambda_{\text{em}} = 575$ nm) traces of RhoB-PDMA sample obtained in run 9.

which seems to correspond to chains terminated by bimolecular combination according to the molecular weight value at the peak maximum (M_p) (A: M_p , main peak = 9700 g mol^{-1} , M_p , shoulder = 18500 g mol^{-1} ; B: M_p , main peak = 8500 g mol^{-1} , M_p , shoulder = 17800 g mol^{-1}). Such longer chains cannot result from the binding of two SH-ended chains (by formation of a disulfide bond) since hydrolysis of the dithiobenzoate moiety does not occur in DMF (anhydrous DMF was used). However, this shoulder represents only ca. 10 wt.% of the sample (*i.e.* 5% of the polymer chains). A similar result was obtained by Donovan et al. [77] for the polymerization of DMA mediated by a dithiobenzoate with an analogous structure to our CTAs, bearing instead a *N,N*-dimethyl propionamide moiety as R group (with an identical $[CTA]_0/[AIBN]_0$ ratio of 5). The authors demonstrated that if the $[CTA]_0/[AIBN]_0$ ratio was increased to 80, the shoulder was completely eliminated (though, the polymerization rate strongly decreased and several

Table 2

Theoretical and experimental M_n and dispersity (D) values for dye-labeled PDMA samples.

Run	Polymer	Conv. (%)	$M_{n,\text{theor}}^a$ (g.mol $^{-1}$)	$M_{n,\text{SEC}}^b$ (g.mol $^{-1}$)	D^b	$M_{n,\text{NMR}}^c$ (g.mol $^{-1}$)	DI_{exp}^d	DI_{theo}^e
2	MG-PDMA	42	15,200	41,600	1.06	n.d.	–	–
3	MG-PDMA	30	2100	9000	1.06	8900	1.0	0.93
7	RhoB-PDMA	61	21,900	n.d.	n.d.	21,200	–	–
8	RhoB-PDMA	39	12,500	18,900	1.07	17,900	1.0	0.91
9	RhoB-PDMA	33	4900	8600	1.11	7800	1.1	0.90

$$^a M_{n,\text{theor}} = \frac{[DMA]_0 \times MW_{\text{DMA}} \times \text{conversion}}{[CTA]_0} + MW_{\text{CTA}}$$

^b Obtained by SEC using 0.05 mol L^{-1} LiBr in DMF as eluent (calibration with PDMA standards).

^c Average value between $M_{n,\text{NMR}}$ values obtained using region B or C (cf. Figs. 4 and 5 and equation (1)).

$$^d DI_{\text{exp}} = M_{n,\text{SEC}}/M_{n,\text{NMR}}$$

$$^e DI_{\text{theo}} = [CTA]_0 / ([CTA]_0 + [\text{initiator}]_0 \times (1 - e^{-k_2})).$$

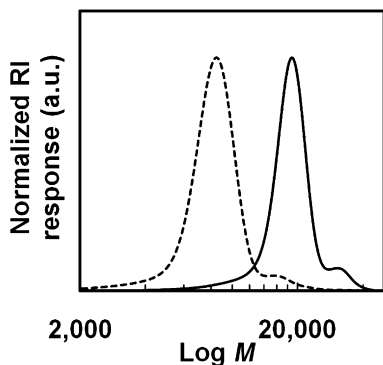


Fig. 3. Comparison of RI traces of SEC chromatograms of RhoB-PDMA samples from run 8 (black line) and run 9 (dotted line).

days were necessary to achieve 67% conversion). In addition, these SEC chromatograms confirmed the presence of MG and RhoB at the polymer chain-end. Indeed, the RI and the UV–visible traces (in the case of MG-PDMA samples) or the RI and the fluorescence traces (in the case of RhoB-PDMA samples) perfectly overlap.

The control of the molecular weights of the MG- and RhoB-labeled PDMA samples was investigated from the SEC analyses and the ^1H NMR spectra. The dispersity determined by SEC was very low ($\bar{D} < 1.2$, Table 2). In the case of MG-PDMA samples, the experimental M_n values were much higher than the calculated $M_{n,\text{theor}}$ (Table 2) which was expected considering the significant amount of impurities in the CTA. In the case of RhoB-PDMA samples, the experimental M_n values were somewhat higher than $M_{n,\text{theor}}$ (Table 2). In fact, the presence of a α -RhoB-chain-end can influence the retention volume as mentioned above [72]. However, the relative comparison between runs 8 and 9 (where $M_{n,\text{theor}}$ is 2.5 times higher in run 8) indicates that experimental M_n values are 2.2–2.3 times higher in run 8 (Table 2 and Fig. 3 that shows a clear shift between the corresponding peaks). These observations confirm that the molecular weights of the RhoB-PDMA samples are

indeed controlled by $[\text{CTA}]_0$ (as expected since RhoB-labeled CTA used in runs 7 to 9 was pure).

After purification by dialysis, the dye-labeled PDMA samples were characterized by ^1H NMR (MG-PDMA: Fig. 4; RhoB-PDMA: Fig. 5). By comparison of the ^1H NMR spectra of the dye-labeled PDMA samples and the corresponding dye-labeled CTA, the presence of MG ethyl propanoyl amide (Fig. 4: aromatic protons, at 7.0–7.8 ppm and protons 1, at ~ 3.2 ppm) and RhoB propanoyl piperazine amide moieties (Fig. 5: protons 3–9, at 6.8–7.8 ppm; protons 1, at ~ 1 ppm and protons 2 and 10) was confirmed at the α -end of the chains, as well as the dithiobenzoate moiety at the ω -end (Fig. 4: MG-PDMA; proton 3' at 7.9 ppm and Fig. 5: RhoB-PDMA; protons 1'-2', between 7.2 and 7.8 ppm and protons 3', at 8 ppm), showing that both chain-ends are preserved after purification by dialysis.

If we consider that all chains are dormant and bear the dye moiety at the α -chain-end, an estimation of M_n of PDMA samples can be obtained by comparison of the integral corresponding to region A (6.8–8.0 ppm) with integrals of region B (2.2–3.4 ppm) or C (1.0–2.0 ppm) using equation (1):

$$M_{n,\text{NMR}} = \left(\frac{I_{\text{B or C}} - n_{\text{B or C, CTA}}}{n_{\text{B or C, DMA}}} \right) \times \frac{I_{\text{A}}}{n_{\text{A, CTA}}} \times \text{MW}_{\text{DMA}} + \text{MW}_{\text{CTA}} \quad (1)$$

where I is the integral value, n_{CTA} and n_{DMA} are respectively the number of CTA and DMA protons in the corresponding region, MW_{DMA} and MW_{CTA} are respectively the molecular weight of DMA and CTA.

The values of $M_{n,\text{NMR}}$ are slightly overestimated since we considered that all chains bear both fragments from the CTA, which is not completely correct due to the presence of some dead chains and some chains initiated by primary radicals from AIBN. However, according to our experimental conditions, we should expect less than 10% of dead chains. Generally, the ratio between absolute M_n values and $M_{n,\text{NMR}}$ values should provide an estimation of dye incorporation (DI). In our case, since it was not possible to get

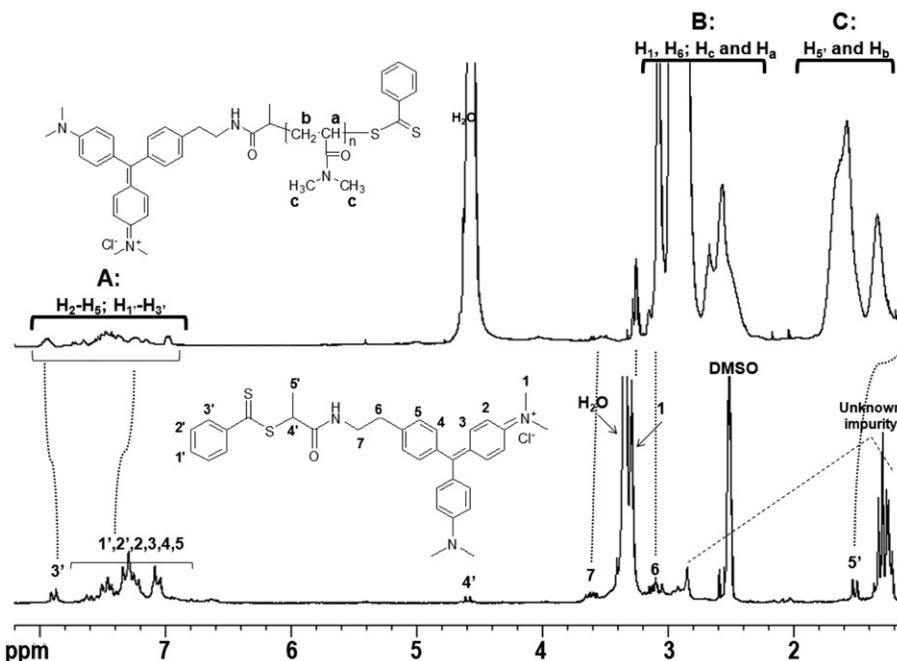


Fig. 4. Comparison of ^1H NMR spectra of MGEDBA ($\text{DMSO}-d_6$, 300 MHz, 27 °C) and MG-PDMA (run 4; $M_{n,\text{SEC}} = 9000 \text{ g mol}^{-1}$; D_2O , 400 MHz, 40 °C).

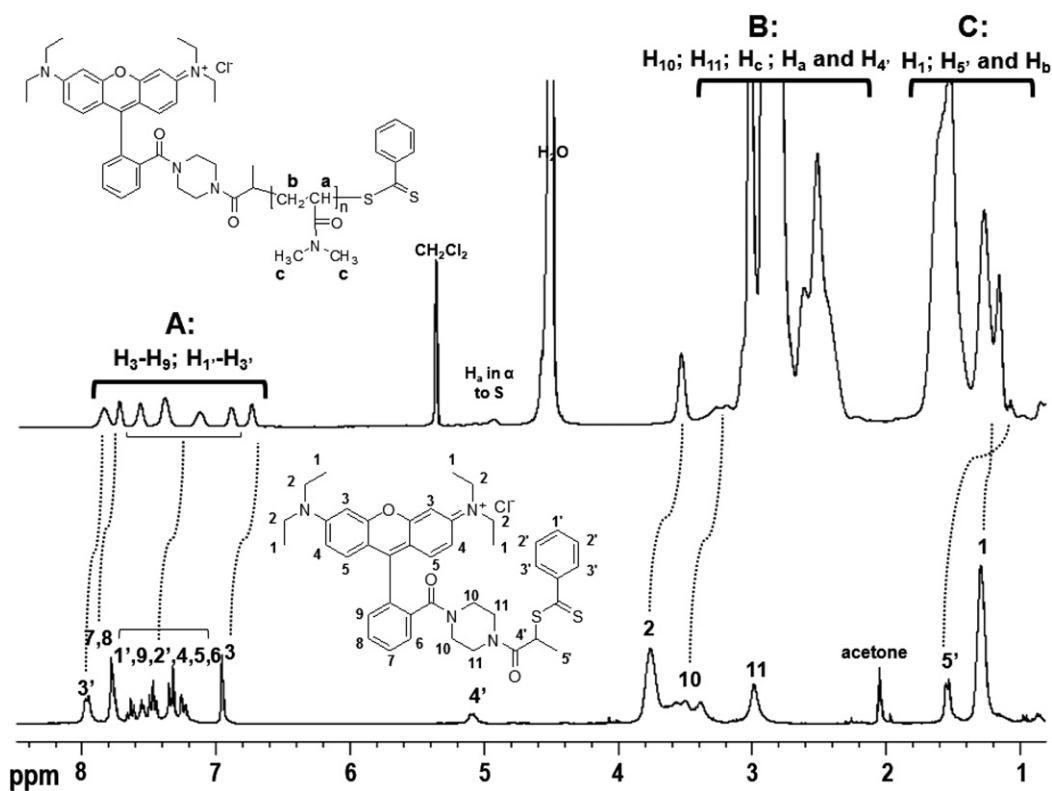


Fig. 5. Comparison of ^1H NMR spectra of RhoBEDBA-3 (acetone- d_6 , 300 MHz, 27 °C) and RhoB-PDMA (run 9; $M_{n, \text{SEC}} = 8600 \text{ g mol}^{-1}$; D_2O , 400 MHz, 40 °C).

absolute M_n values, the relative $M_{n, \text{SEC}}$ values were used. However, since both $M_{n, \text{NMR}}$ and $M_{n, \text{SEC}}$ values are overestimated, the dye incorporation values have to be considered with caution (DI_{exp} in Table 2). Although there are some non-labeled chains (less than 10% considering the used $[\text{CTA}]_0/[\text{AIBN}]_0$ ratio, the temperature and the polymerization times), for most applications these non-labeled chains do not interfere with the results (it is often necessary to mix labeled with non-labeled chains otherwise fluorescence is too high).

These results confirm that the novel high valued water-soluble dye-labeled dithiobenzoates, MGEDBA and RhoBEDBA (with a very polar and charged structure), are as efficient as *t*BDB (a simple CTA) to control the RAFT polymerization of DMA. Although CTA purity has a strong influence on RAFT polymerization kinetics, we got a very satisfying control over molecular weights and chain-end functionalization of the RhoB-labeled PDMA samples.

3.4. Photophysical properties of dye-labeled CTAs and corresponding polymers

The absorption spectra of MG-ethylammonium chloride (2), MGEDBA (3) and MG-PDMA (run 4) were traced in acidified ethanol (Fig. 6). Being a planar or nearly planar molecule, MG presents two types of absorption bands, one polarized along the *x* direction and other along the *y* direction. So, as expected, the maximum absorption band of the MG derivatives and MG-labeled polymer is located at *ca.* 620 nm, which corresponds to the promotion of an electron from the nonbonding molecular orbital (NBMO) of one of the nitrogen atoms to the lowest antibonding orbital, producing an excited state with a high electron density on the central carbon atom (*x*-band transition) ($\lambda_{\text{abs}}^{\text{max}} = 616.5 \text{ nm}$; $\epsilon_{\text{abs}}^{\text{max}} = 148\,900$) [39]. The *y* band that arises from excitation of an electron from the

second highest occupied bonding orbital to the lowest vacant orbital and involves migration from the phenyl ring to the rest of the system [82] appears at around $\lambda_{\text{abs}}^{\text{max}} = 425 \text{ nm}$. Only a slight difference of a few nm in the maximum absorbance wavelength can be detected between the various derivatives (Table 3) and it is very close to the value of non-modified MG ($\lambda_{\text{abs}}^{\text{max}} = 616.5 \text{ nm}$ [39]), showing that the derivatization of MG led to almost no changes in the molecular orbital energy levels. Molar absorption coefficients of

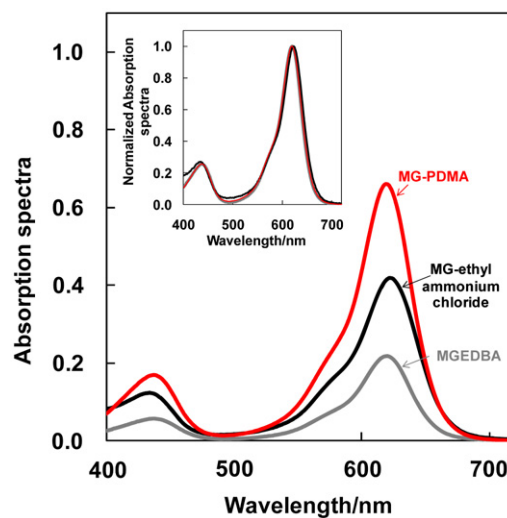


Fig. 6. Absorption spectra of MG-ethylammonium chloride (2, black, $C_{\text{app}} = 4.04 \times 10^{-5} \text{ mol L}^{-1}$), MGEDBA (3, grey, $C_{\text{app}} = 9.67 \times 10^{-5} \text{ mol L}^{-1}$) and MG-PDMA (run 4, red, $[\text{polymer}] = 1.58 \times 10^{-5} \text{ mol L}^{-1}$). Insert: normalized spectra indicating that the maximum absorption wavelength remains the same. (For interpretation of the references to colour in this figure legend, the reader is referred to the web version of this article.)

Table 3
Photophysical properties of dye derivatives and dye-labeled polymers.

Derivative	$\lambda_{\text{abs}}^{\text{max}}/\text{nm}$	$\epsilon_{\text{abs}}^{\text{max}}/10^4 \text{ mol}^{-1} \text{ L cm}^{-1}$	$\lambda_{\text{em}}^{\text{max}}/\text{nm}$	ϕ_{F}	Decay parameters							
					a_1	τ_1/ns	a_2	τ_2/ns	a_3	τ_3/ns	$\langle\tau\rangle^{\text{b}}$	χ^2
2	622	2.8 ^a	—	—	—	—	—	—	—	—	—	—
MGEDBA	620	0.41 ^a	—	—	—	—	—	—	—	—	—	—
MG-PDMA	619	8.4	—	—	—	—	—	—	—	—	—	—
4	562	8.7 ± 0.9	583	0.54	1	1.97	—	—	—	—	1.97	1.02
RhoBEDBA	563	9.3 ± 0.4	586	0.21	5.27	2.00	11.6	1.03	22.4	0.32	0.76	0.91
RhoB-PDMA	562	9.5 ± 0.2	582	0.58	1	2.12	—	—	—	—	2.12	1.03

^a Apparent value, since the real concentration in chromophore is unknown.

^b Calculated by $\langle\tau\rangle = \frac{\sum_i a_i \tau_i}{\sum_i a_i}$.

MG-ethylammonium chloride (**2**) and MGEDBA (**3**) were obtained from the plots of maximum absorbance as a function of concentration using the Beer–Lambert law (Table 3). However, since impurities remained in these products, the values were much lower than expected for this kind of compounds ($\epsilon_{\text{abs}}^{\text{max}} = 10.6 \times 10^4 \text{ mol}^{-1} \text{ L cm}^{-1}$) [83], because the apparent concentration of the compound did not correspond to its real concentration. On the other hand, the molar absorption coefficient value obtained for MG-PDMA is much closer to that of MG, showing that after purification by dialysis most of the impurities were removed. It is noteworthy that in the case of both MGEDBA and MG-PDMA, the band corresponding to the absorption of the dithiobenzoate moiety ($\lambda_{\text{abs}}^{\text{max}} = 500\text{--}530 \text{ nm}$) could not be observed on the spectrum, which is due to the fact that this chromophore has a much lower molar absorption coefficient value ($\epsilon_{\text{abs}}^{\text{max}} < 100 \text{ mol}^{-1} \text{ L cm}^{-1}$) [84].

Fig. 7 shows absorption and fluorescence emission spectra of RhoB piperazine amide (**4**), RhoBEDBA (**5**) and RhoB-PDMA (run 9) solutions in acidified ethanol (for simplicity, the absorption and fluorescence emission maxima were normalized to unity). As it can be observed, the two RhoB derivatives and RhoB-PDMA present very similar absorption and fluorescence maximum wavelengths (Table 3), showing that both the modification of the RhoB dye and the attachment to a polymer chain do not cause any significant change in its photophysical properties.

The absorption spectra of RhoB piperazine amide (**4**), RhoBEDBA (**5**) were traced at several dye concentrations (10^{-6} to $10^{-5} \text{ mol L}^{-1}$) and the plots of maximum absorbance as a function of concentration were linear for both derivatives (results not shown). Hence, molar absorption coefficients of these derivatives as well as of

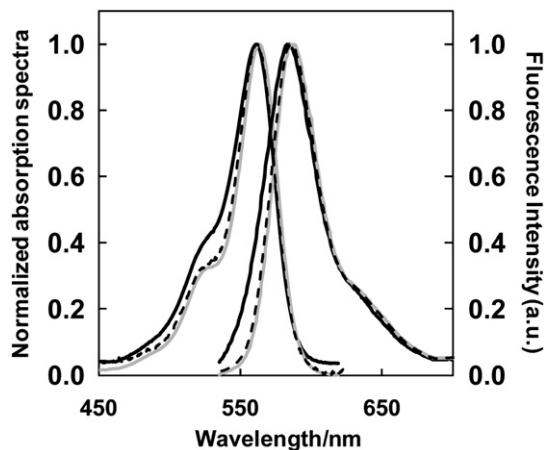


Fig. 7. Normalized absorption and emission ($\lambda_{\text{exc}} = 530 \text{ nm}$) spectra of RhoB piperazine amide (**4**, black lines), RhoBEDBA (**5**, grey lines) RhoB-PDMA (run 9, dotted lines) solutions in ethanol at OD = 0.1.

RhoB-PDMA were determined using Beer–Lambert law. Those values are slightly lower than of the parent RhoB ($\epsilon_{\text{abs}}^{\text{max}} = 11.1 \times 10^4 \text{ mol}^{-1} \text{ L cm}^{-1}$) [38], however they are in agreement with previously reported values [49]. As in the case of MGEDBA and MG-PDMA, the band corresponding to the dithiobenzoate moiety cannot be detected due to its much lower molar absorption coefficient value.

The fluorescence quantum yields of these RhoB derivatives and of RhoB-PDMA were determined by comparing their fluorescence emission spectra with that of Rhodamine 101 in acidified ethanol using equation (2):

$$\phi_{\text{F}} = \frac{A_{\text{Rho101}}}{A} \times \frac{F}{F_{\text{Rho101}}} \times \left(\frac{n_{\text{solvent}}}{n_{\text{EtOH}}} \right)^2 \times \phi_{\text{F, Rho 101}} \quad (2)$$

where ϕ_{F} is the fluorescence quantum yield, A is the absorbance at the excitation wavelength ($A \leq 0.1$), F is the area under the

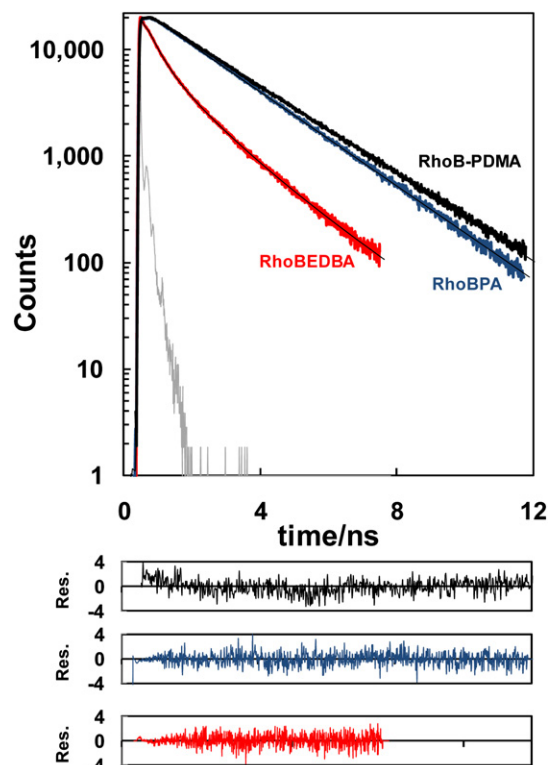


Fig. 8. Fluorescence decay curves for RhoB-PDMA (run 9, black), RhoBPA (blue) and RhoBEDBA (red) solutions in ethanol ($10^{-6} \text{ mol L}^{-1}$). The solutions were excited at 570 nm and emission was monitored at 585 nm. The solid black line represents the best fit to the data. The lamp profile is also shown (light grey line). The weighted residuals are shown below the decay curves. (For interpretation of the references to colour in this figure legend, the reader is referred to the web version of this article.)

corrected emission curve, and n is the refractive index of the used solvents.

Solutions were prepared in order to have an optical density of 0.1 at the excitation wavelength ($\lambda_{\text{exc}} = 530$ nm). Although the fluorescence quantum yield value obtained for **4** is very similar to the reported value for RhoB in its cationic form, a much lower value was observed for RhoBEDBA (Table 3). The main reason must be the fluorescence quenching caused by the presence of a dithiobenzoate group. [84] In fact, while the fluorescence decay of **4** could be fitted with a single exponential function (with $\chi^2 < 1.2$ and homogeneously distributed weighted residuals and autocorrelation of residuals), a sum of three exponentials was necessary for the fitting of the fluorescence decay of RhoBEDBA (Fig. 8). It is however remarkable that the fluorescence decay of the RhoB-PDMA polymer sample is also monoexponential, meaning that the polymer chain allows RhoB to be sufficiently far away from the dithiobenzoate moiety to avoid intra-molecular quenching (at these diluted polymer concentrations, the intermolecular quenching is very unlikely). The lifetime of RhoB-PDMA is slightly longer than that of RhoBPA because attaching the dye to a polymer chain reduces in some extent its radiationless deactivation processes.

4. Conclusions

We describe the synthesis of two novel cationic RAFT agents, one labeled with a Malachite Green (MG) dye and another with a Rhodamine B (RhoB) dye. First, MG and RhoB derivatives bearing an amino functional group were synthesized. In the case of RhoB, a secondary amino derivative was prepared and for MG, we presented an original one-pot synthetic route. Then, a MG-labeled dithiobenzoate (MGEDBA) was prepared in a straightforward manner using a convergent approach by reaction of MG-ethylammonium chloride (**2**) with a precursor dithiobenzoate bearing an activated ester function (**1**). However, the analogous reaction with RhoB amino derivative led to a mixture of dithiobenzoate and thioamide derivatives, suggesting that secondary amines have almost the same reactivity with respect to the dithiobenzoate moiety compared to the activated ester moiety. An alternative linear approach was then used, yielding the RhoB-labeled RAFT agent (RhoBEDBA) with complete conversion.

The purification of these dye-labeled CTAs was very challenging because of their dual nature (aromatic and ionic). Indeed, elimination of all impurities from the MGEDBA sample was not possible. On the contrary, it was possible to fully purify RhoBEDBA (>98% by silica gel chromatography) keeping a satisfactory yield (58%).

Both MGEDBA and RhoBEDBA were efficient CTAs to control the RAFT homopolymerization of DMA, since in all cases the resulting polymer samples presented low dispersities ($\bar{M}_w/\bar{M}_n < 1.2$) and both chain-ends were preserved. In some cases, the presence of impurities slowed down the polymerization kinetics. However, when a very pure RhoBEDBA sample was employed, the time evolution of monomer conversion was very similar to that observed when a simple CTA, tBDB, was used.

Finally, we showed that the attachment of RhoB and MG to the PDMA polymer chain-end did not influence the photophysical properties of these dyes. Therefore, these new dye-labeled RAFT agents can be used to prepare various polymers and especially water-soluble ones, to study their conformation and dynamics in solution or at interfaces using fluorescence methods, or to get labeled probes for imaging and diagnosis purposes. Several thermosensitive block copolymers have been prepared from the MG- and RhoB-labeled PDMA homopolymers; their synthesis as well as fluorescence studies in aqueous solutions will be reported in a further publication.

Acknowledgment

The authors thank the Portuguese NMR Network (IST-UTL Center) for providing access to the NMR facilities, Dr. Michel Becchi (CCMP, IBCP, SFR Biosciences Gerland-Lyon Sud UMS344/US8, Lyon, France) for carrying out mass spectrometry, Mr. Vincent Martin (Laboratoire des Matériaux Organiques à Propriétés Spécifiques, Solaize, France) for the determination of specific refractive index increment, Dr. Aleksander Fedorov for the time-resolved fluorescence measurements and Dr. Željko Petrovski and Dr. Pedro Góis for organic experimental help and advice. Mariana Beija thanks Fundação para a Ciência e Tecnologia for her PhD grant (SFRH/BD/18562/2004).

Supporting Information

Assignments of ^1H and ^{13}C NMR peaks of MG and RhoB derivatives; ^1H , ^{13}C NMR and MS spectra of MGEDBA and RhoBEDBA, MALDI-ToF MS spectra (reflectron mode) of final polymerization mixtures of runs 5 and 6.

Appendix. Supplementary material

Supplementary data associated with this article can be found, in the online version, at doi:10.1016/j.polymer.2011.10.041

References

- Piçarra S, Gomes PT, Martinho JMG. *Macromolecules* 2000;33:3947–50.
- Laukkanen A, Winnik FM, Tenhu H. *Macromolecules* 2005;38:2439–48.
- Relógio P, Martinho JMG, Farinha JPS. *Macromolecules* 2005;38:10799–811.
- Winnik MA. *Acc Chem Res* 1985;18:73–9.
- Beija M, Relógio P, Charreyre MT, da Silva AMG, Brogueira P, Farinha JPS, et al. *Langmuir* 2005;21:3940–9.
- Callahan J, Kopecek J. *Biomacromolecules* 2006;7:2347–56.
- Kim K, Lee M, Park H, Kim JH, Kim S, Chung H, et al. *J Am Chem Soc* 2006;128:3490–1.
- Charreyre MT, Mandrand B, Martinho JMG, Relógio P, Farinha JPS. Fluorescent polymers soluble in an aqueous solution and a method for the production thereof. Biomérieux S.A. Centre National de la Recherche Scientifique; Instituto Superior Técnico; 2007. WO2007003781.
- Chen M, Ghiggino KP, Mau AWH, Rizzardo E, Thang SH, Wilson GJ. *Chem Commun*; 2002:2276–7.
- Beija M, Charreyre M-T, Martinho JMG. *Prog Polym Sci* 2011;36:568–602.
- Farinha JPS, Martinho JMG. *J Phys Chem C* 2008;112:10591–601.
- Barner-Kowollik C. *Handbook of RAFT polymerization*. Weinheim: Wiley-VCH; 2008.
- Chiefari J, Chong YK, Ercole F, Krstina J, Jeffery J, Le TPT, et al. *Macromolecules* 1998;31:5559–62.
- Willcock H, O'Reilly RK. *Polym Chem* 2010;1:149–57.
- Nakayama M, Okano T. *Biomacromolecules* 2005;6:2320–7.
- Favier A, Ladavière C, Charreyre M-T, Pichot C. *Macromolecules* 2004;37:2026–34.
- Scales CW, Convertine AJ, McCormick CL. *Biomacromolecules* 2006;7:1389–92.
- Segui F, Qiu XP, Winnik FM. *J Polym Sci Part A Polym Chem* 2008;46:314–26.
- Zhu J, Zhu XL, Cheng ZP, Liu F, Lu JM. *Polymer* 2002;43:7037–42.
- Li Y, Yang JW, Benicewicz BC. *J Polym Sci Part A Polym Chem* 2007;45:4300–8.
- Chen M, Ghiggino KP, Thang SH, White J, Wilson GJ. *J Org Chem* 2005;70:1844–52.
- Zhou NC, Lu LD, Zhu XL, Yang XJ, Wang X, Zhu J, et al. *Polym Bull* 2006;57:491–8.
- Zhou NC, Zhu J, Zhang ZB, Zhu XL. *E-Polymers*; 2007.
- Fu J, Cheng ZP, Zhou N, Zhu J, Zhang W, Zhu X. *Polymer* 2008;49:5431–8.
- Zhu J, Zhu XL, Zhou D, Chen JY, Wang XY. *Eur Polym J* 2004;40:743–9.
- Prazeres TJV, Beija M, Farinha JPS, Charreyre MT, Martinho JMG. *Polymer* 2010;51:355–67.
- Zhou N, Lu L, Zhu J, Yang X, Wang X, Zhu X, et al. *Polymer* 2007;48:1255–60.
- Chen M, Ghiggino KP, Mau AWH, Sasse WHF, Thang SH, Wilson GJ. *Macromolecules* 2005;38:3475–81.
- Zhou D, Zhu XL, Zhu J, Hu LH, Cheng ZP. *E-Polymers*; 2006.
- Wan XM, Zhu XL, Zhu J, Zhang ZB, Cheng ZP. *J Polym Sci Part A Polym Chem* 2007;45:2886–96.
- Zhou D, Zhu X, Zhu J, Cheng ZP. *J Polym Sci Part A Polym Chem* 2008;46:6198–205.

- [32] Such GK, Evans RA, Davis TP. *Macromolecules* 2006;39:9562–70.
- [33] Mertoglu M, Laschewsky A, Skrabania K, Wieland C. *Macromolecules* 2005;38:3601–14.
- [34] Chen M, Ghiggino KP, Mau AWH, Rizzardo E, Sasse WHF, Thang SH, et al. *Macromolecules* 2004;37:5479–81.
- [35] Chen M, Ghiggino KP, Thang SH, Wilson GJ. *Angew Chem Int Ed* 2005;44:4368–72.
- [36] Chen M, Ghiggino KP, Launikonis A, Mau AWH, Rizzardo E, Sasse WHF, et al. *J Mater Chem* 2003;13:2696–700.
- [37] Zana R. Fluorescence studies of amphiphilic block copolymers in solution. In: Alexandridis P, Lindman B, editors. *Amphiphilic block copolymers - self-assembly and applications*. Amsterdam: Elsevier; 2000.
- [38] Arbeloa FL, Arbeloa TL, Estevez MJT, Arbeloa IL. *J Phys Chem* 1991;95:2203–8.
- [39] Green FJ. *The Sigma-Aldrich Handbook of stains, dyes and indicators*. Aldrich Chem Co Library; 1990.
- [40] Valeur B. *Molecular fluorescence - principles and applications*. Weinheim: WileyVCH; 2002.
- [41] Farinha JPS, Charreyre MT, Martinho JMG, Winnik MA, Pichot C. *Langmuir* 2001;17:2617–23.
- [42] Fonseca T, Relógio P, Martinho JMG, Farinha JPS. *Langmuir* 2007;23:5727–34.
- [43] Prazeres TJV, Farinha JPS, Martinho JMG. *J Phys Chem C* 2008;112:16331–9.
- [44] Martinho JMG, Prazeres TJV, Moura L, Farinha JPS. *Pure Appl Chem* 2009;81:1615–34.
- [45] Moura LM, Martinho JMG, Farinha JPS. *Chem PhysChem* 2010;11:1749–56.
- [46] Romão RIS, Beija M, Charreyre M-T, Farinha JPS, Gonçalves da Silva AMPs, Martinho JMG. *Langmuir* 2010;26:1807–15.
- [47] Bathfield M, D'Agosto F, Spitz R, Charreyre MT, Delair T. *J Am Chem Soc* 2006;128:2546–7.
- [48] Favier A, Charreyre MT, Chaumont P, Pichot C. *Macromolecules* 2002;35:8271–80.
- [49] Nguyen T, Francis MB. *Org Lett* 2003;5:3245–8.
- [50] Van Geet AL. *Anal Chem* 1968;40:2227–9.
- [51] Hoffman RE, Becker ED. *J Magn Reson* 2005;176:87–98.
- [52] Marquardt DW. *J Soc Ind Appl Math* 1963;11:431.
- [53] Bathfield M, Daviot D, D'Agosto F, Spitz R, Ladavière C, Charreyre M-T, et al. *Macromolecules* 2008;41:8346–53.
- [54] Pratt EF, Green LQ. *J Am Chem Soc* 1953;75:275–8.
- [55] Barker CC, Hallas G, Bride MH, Stamp A. *J Chem Soc*; 1961:1285.
- [56] Ritchie CD, Sager WF, Lewis ES. *J Am Chem Soc* 1962;84:2349–56.
- [57] Armstrong L, Jones AM. *Dyes Pigm* 1999;42:65–70.
- [58] Hallas G, Grocock DE, Hepworth JD. *J Soc Dyers Colourists* 1970;86:200.
- [59] Castelino RW, Hallas G. *J Chem Soc B: Physical Organic*; 1971:1471–3.
- [60] Hallas G, Paskins KN, Waring DR, Humpston JR, Jones AM. *J Chem Soc Perk Trans* 1977;2:450–6.
- [61] Cho BP, Blankenship LR, Moody JD, Doerge DR, Beland FA, Culp SJ. *Tetrahedron* 2000;56:7379–88.
- [62] Kimura K, Yokota G, Yokoyama M, Uda RM. *Macromolecules* 2001;34:2262–8.
- [63] DeFina SC, Dieckmann TJ. *Labelled Compd Radiopharm* 2002;45:241–8.
- [64] Djuric S, Venit J, Magnus P. *Tetrahedron Lett* 1981;22:1787–90.
- [65] Beija M, Afonso CAM, Martinho JMG. *Chem Soc Rev* 2009;38:2410–33.
- [66] Kim HN, Lee MH, Kim HJ, Kim JS, Yoon J. *Chem Soc Rev* 2008;37:1465–72.
- [67] Albeit ESI-MS and ¹³C NMR techniques are not quantitative methods, since the two molecular structures are very similar and the considered carbon is of the same nature (C=S), a similar ESI-MS response and a comparable relaxation for ¹³C NMR should be expected.
- [68] Kopecek J, Sprincl L, Bazilova H, Vacik J. *J Biomed Mater Res* 1973;7:111–21.
- [69] Chiari M, Cretich M, Consonni R. *Electrophoresis* 2002;23:536–41.
- [70] Relógio P, Charreyre MT, Farinha JPS, Martinho JMG, Pichot C. *Polymer* 2004;45:8639–49.
- [71] Relógio P. *Water-soluble associative polymers: synthesis and photophysical study of poly(N, N-dimethylacrylamide) and poly(N-acryloylmorpholine)*. Química, vol. PhD. Lisbon: Universidade Técnica de Lisboa; 2006.
- [72] Bathfield M. *Synthèse d'agents de contrôle originaux pour l'obtention de copolymères alpha-fonctionnels par le procédé RAFT. Application à l'élaboration de particules à chevelure contrôlée*. vol. Doctorat. Lyon: Université Claude Bernard - Lyon 1; 2006.
- [73] ten Cate MGJ, Rettig H, Bernhardt K, Borner HG. *Macromolecules* 2005;38:10643–9.
- [74] Plummer R, Goh YK, Whittaker AK, Monteiro MJ. *Macromolecules* 2005;38:5352–5.
- [75] Teodorescu M, Matyjaszewski K. *Macromolecules* 1999;32:4826–31.
- [76] Kobayashi M, Ishizone T, Nakahama S. *Macromolecules* 2000;33:4411–6.
- [77] Donovan MS, Lowe AB, Sumerlin BS, McCormick CL. *Macromolecules* 2002;35:4123–32.
- [78] Schierholz K, Givehchi M, Fabre P, Nallet F, Papon E, Guerret O, et al. *Macromolecules* 2003;36:5995–9.
- [79] Li YT, Lokitz BS, McCormick CL. *Macromolecules* 2006;39:81–9.
- [80] Gondi SR, Vogt AP, Sumerlin BS. *Macromolecules* 2007;40:474–81.
- [81] Kirkland SE, Hensarling RM, McConaughy SD, Guo Y, Jarrett WL, McCormick CL. *Biomacromolecules* 2008;9:481–6.
- [82] Duxbury DF. *Chem Rev* 1993;93:381–433.
- [83] Herz ML. *J Am Chem Soc* 1975;97:6777–85.
- [84] Farinha JPS, Relógio P, Charreyre MT, Prazeres TJV, Martinho JMG. *Macromolecules* 2007;40:4680–90.